Sea-level trends in the Australian region

a UNIVERSITY of TASMANIA AUSTRALIA b TECHNISCHE UNIVERSITÄT MÜNCHEN c CSIRO d ACE CRC ANTARCTIC CLIMATE & ECOSYSTEMS COOPERATIVE RESEARCH CENTRE e UNSW AUSTRALIA

Sam Royston,[*,a] Christopher Watson,[a] Matt King,[a] Marcello Passaro,[b] Benoit Legresy,[c,d] John Church[e]

Introduction

Sea-level variability differs between the open ocean and over the shelf due to the expression of different oceanographic processes(1). This can result in different sea-level trends observed by satellite altimeters in the open ocean and tide gauges at the coast. Many sea-level reconstruction techniques(2,3,4) use tide gauge data as a proxy to reconstruct spatially coherent modes of open ocean sea level variability and regional projections of sea-level change are calculated from global models.

We investigate the variability of sea-level trend between the open ocean and the coast around Australia, using recent improvements in coastal altimetry corrections (range waveform re-tracking, wet tropospheric correction and improved tide models).

Data

We derive sea surface height anomaly (SSHA) time series for 3391 along-track locations for satellite altimetry data from Jason-1 and Jason-2/OSTM (2002—2015). We compare time series with default ("standard") altimetry corrections (from the Level 3 DUACS product in the open ocean) against time series with corrections specifically designed for coastal environments ("coastal")(5,6,7,8) using the RADS database(9). Tide gauge data is monthly mean RLR from PSMSL.

"Open ocean" here refers to along-track points within the EEZ of Australia, generally defined at 300 km from the Australian coast. The "coastal" region is defined as 50 km from the Australian coast.

Ref. name	Region	Corrections	Tide model	Noise model
Open ocean, standard corr.	Open ocean	Range: MLE4 Wet tropo: radiometer + model	GOT	White; coloured
Coastal region, standard corr.	**Coastal**	Range: MLE4 Wet tropo: radiometer + model	GOT 4.10c	Coloured
Coastal region, standard with FES tides	Coastal	Range: MLE4 Wet tropo: radiometer + model	**FES 2014b**	Coloured
Coastal region, coastal corr.	Coastal	Range: **ALES** Wet tropo: **GPD+**	FES 2014b	Coloured
Tide gauge with GIA VLM	Tide gauge	Hydrostatic IBE, nodal long-period equilibrium tides, VLM from ICE-6G	Harmonic analysis	Coloured
Tide gauge with SONEL VLM	Tide gauge	As above, with VLM from SONEL GPS processing	Harmonic analysis	Coloured

Table 1. Data sets compared in this analysis

Method

Noise model {white, AR(1), ARFI(1,*d*), power-law, GGM}

Bias

Linear trend in time

Periodic signals

Climate indices (DCI, ICI)

→ *Hector*[13] MLE regression → Best fit coefficients; Score metrics (min(log(L)), AIC, BIC)

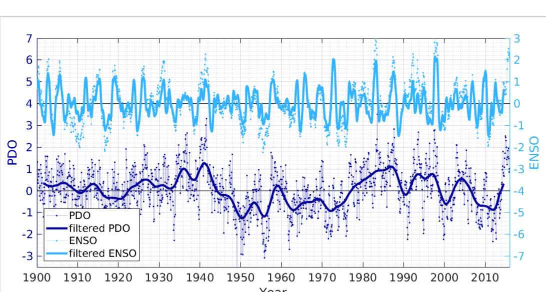

Figure 1. Climate indices: PDO and ENSO indices (dots) and the filtered DCI and ICI (solid lines)

Linear sea-level trends from short observations can be affected by natural decadal variability(10). We use the Multi-variate El Niño Southern Oscillation Index(11) (ENSO MEI) and Pacific Decadal Oscillation(12) (PDO) index as proxies for Pacific climate variability and apply filters to separate a decadal climate index (DCI) from inter-annual climate index (ICI; Fig 1). The standard SSHA time series show ~19% variance explained by a mode highly correlated to ENSO (Fig 2).

Data Sources

DUACS Altimetry: now CMEMS marine.copernicus.eu
RADS: TUDelft rads.tudelft.nl/rads/rads.shtml ; github.com/remkos/rads
ALES: NASA PODAAC ftp://podaac-ftp.jpl.nasa.gov/allData/coastal_alt/L2/ALES/
GPD+: CTOH, AVISO www.aviso.altimetry.fr/en/data/products/auxiliary-products/wet-tropospheric-correction.html
PSMSL: psmsl.org   SONEL: sonel.org
PDO: ftp://ftp.atmos.washington.edu/mantua/pnw_impacts/INDICES/
MEI: www.esrl.noaa.gov/psd/enso

References

1. Vinogradov and Ponte (2011) JGR 116 C07006 doi:10.1029/2011JC007034
2. Church and White (2011) Surv Geophys 32 pp 585—602 doi:10.1007/s10712-011-9119-1
3. Jevrejeva et al (2014) Glob Plan Change 113 doi:10.1016/j.gloplacha.2013.12.004
4. Dangendorf et al (2017) PNAS 114 (23) pp 5946—5951 doi: 10.1073/pnas.1616007114
5. Passaro et al. (2014) Remote Sens Env 145 pp. 173–189 doi:10.1016/j.rse.2014.02.008
6. Fernandes et al (2015) Remote Sens Env 169 pp. 50—74 doi:10.1016/j.rse.2015.07.023
7. Fernandes and Lazaro (2016) Remote Sens 8(10) pp. 851 doi:10.3390/rs8100851
8. Carrere et al (2016) ESA Living Planet Conference
9. Scharroo et al (2013) Proc. Symposium 20 Years Prog. Radar Altimetry, ESA Pub.
10. Zhang and Church (2012) GRL 39 L21701
11. Wolter and Timlin (2011) Intl. J. Climatology 31 pp. 1074—1087 doi:10.1002/joc.2336
12. Mantua et al (1997) BAMS 78 pp. 1069—1079 doi:10.1175/1520-0477(1997)078<1069
13. Bos et al (2013) J Geod 87(4) pp. 351—360 doi:10.1007/s00190-012-0605-0

Acknowledgements
Thanks to Machiel Bos for modifications to the Hector MLE software. Funding from the Australian Research Council Discovery Project DP150100615 and Future Fellows program, Australian Government.

Results

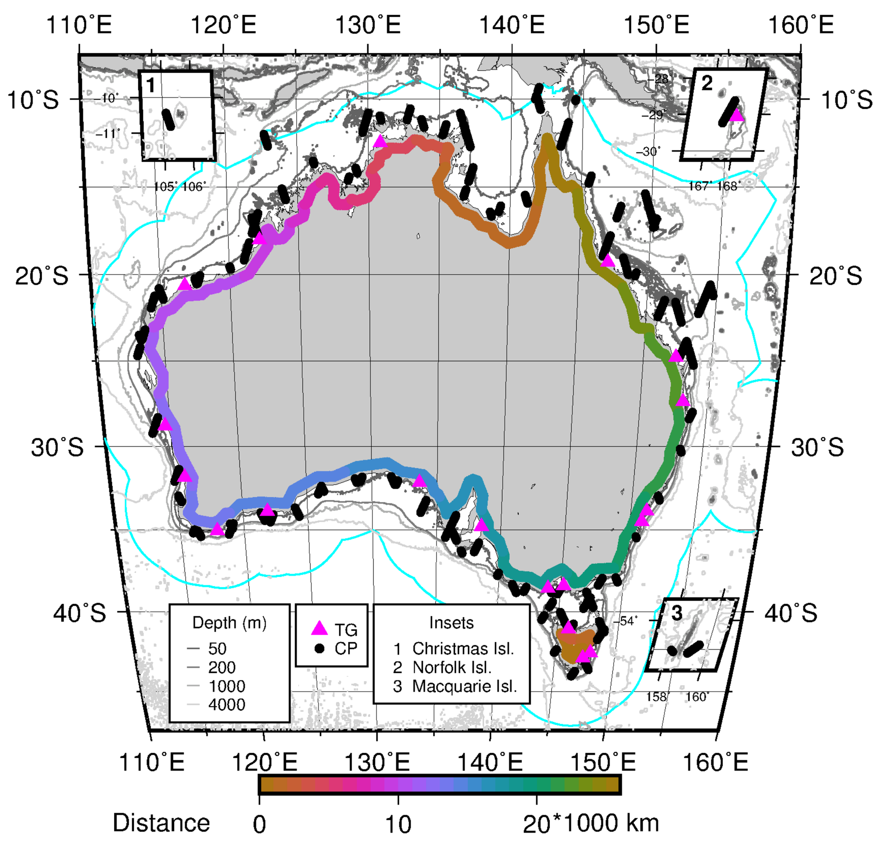

Figure 2. Context of distance around the Australian coastline, counter-clockwise from Torres Strait. Black dots are "coastal region" comparison points, cyan line shows "open ocean region".

Influence of climate on sea level

Including climate indices in the regression highlights a strong negative relationship to both decadal and inter-annual variability from the Indonesian throughflow, along the North West Shelf and on the continental shelf to the Great Australian Bight, as the sea-level disturbance propagates as a coastally-trapped wave. ENSO-related variability is positively correlated (with no lag) in the Coral Sea and GBR where westward-propagating waves can penetrate the Fiji Basin and enter the Coral Sea. The relation at the coast along the Great Barrier Reef reverses, such that the inter-annual variability (ICI) regression coefficients at tide gauges are negative.

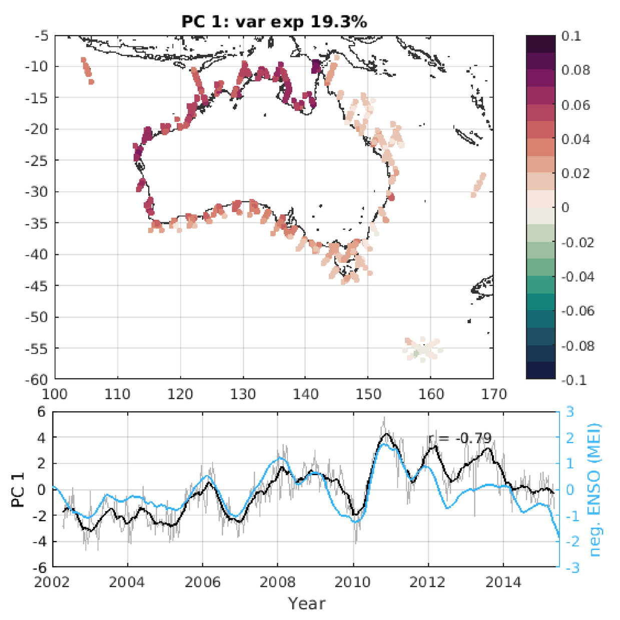

Figure 3. Principal component analysis on the coastal region, standard altimetry data shows the leading mode of variability correlates well with the multi-variate ENSO index

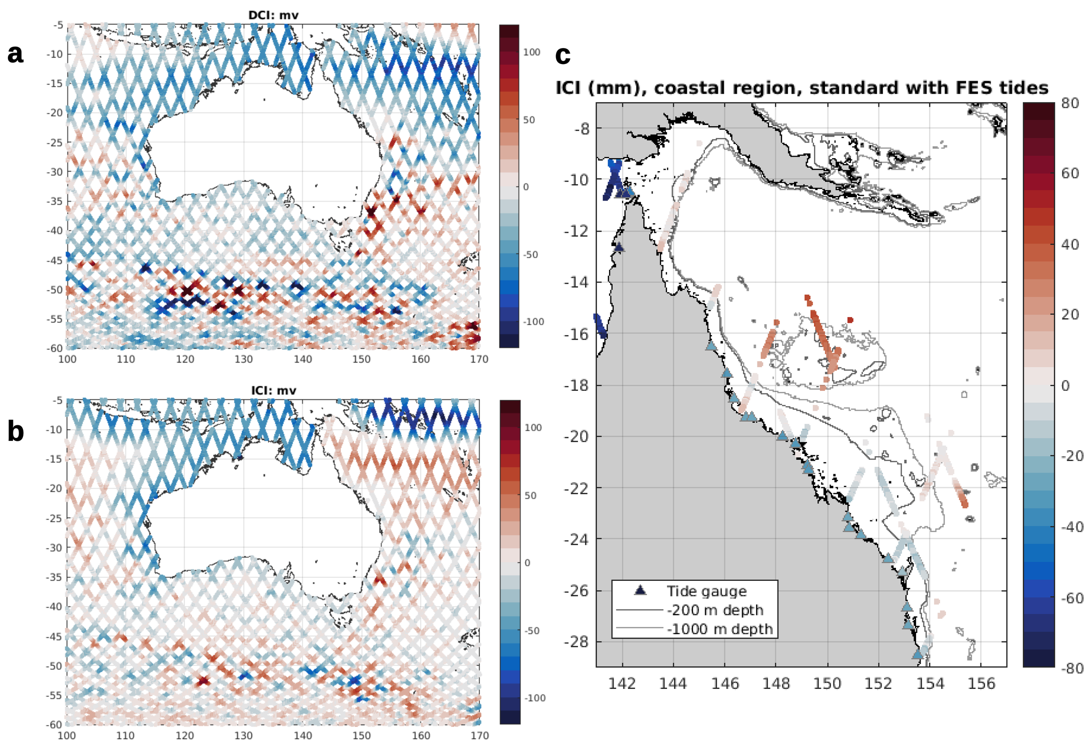

Figure 4. Coefficients (mm) of the multi-variate regression for (a) DCI (open ocean standard SSHA with coloured noise); (b) ICI (open ocean standard SSHA with coloured noise); (c) ICI (coastal region, standard corrections with FES tides).

Sea level trend and its uncertainty

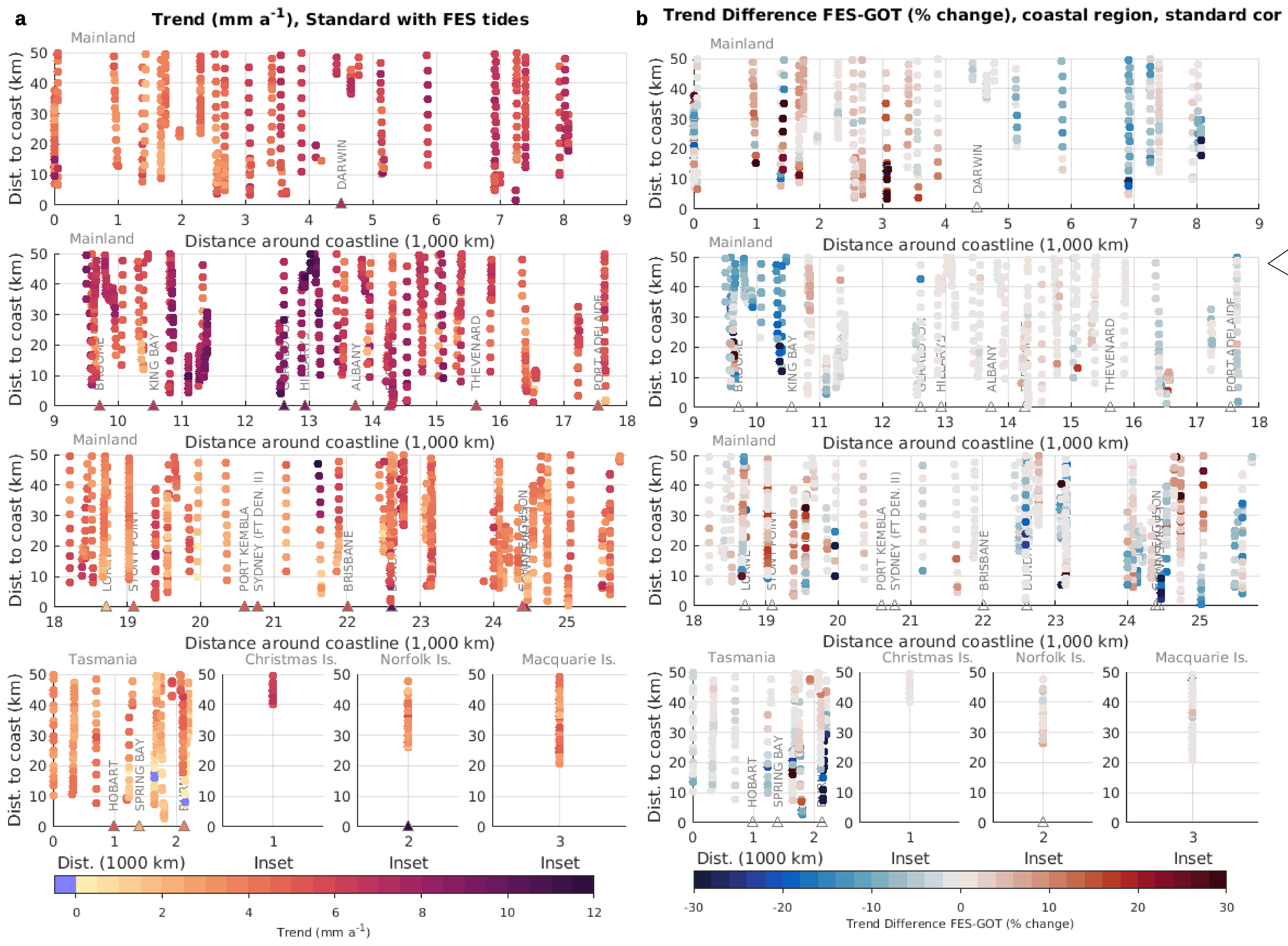

Figure 5. Trend (mm a-1) around the Australian coastal region: (a) standard corrections with FES tides; (b) difference (%) due to applying FES tidal correction rather than GOT

There are spatially coherent patterns in sea-level trend around the Australian coast, with the largest trend occurring in the East Australian and Leeuwin Currents and the smallest trend occurring on the continental shelf of the south-west coast. But the trend is not, in general, correlated with distance from the coast or bathymetry.

FES tidal correction leads to significant differences in the trend (and its uncertainty; Fig 7), compared to GOT, extending out along the continental shelf

Coastal altimetry corrections leads to a generally higher trend. The differences do not correlate with distance from coast or completeness.

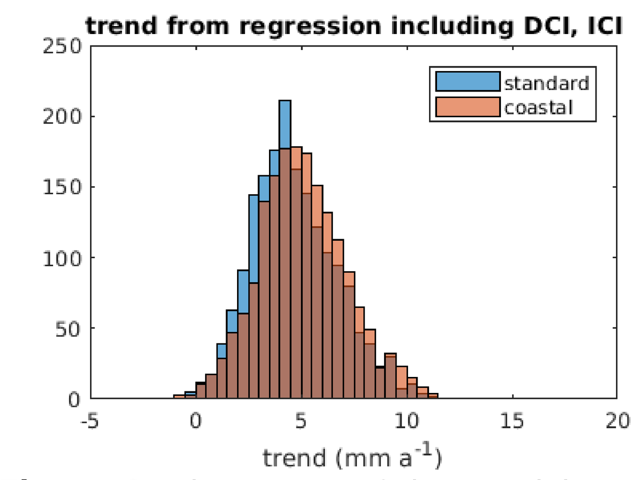

Figure 6. Histograms of the trend (mm a-1) in the coastal region, comparing the standard corrections with FES tides to the coastal correction

Trend (mm a^{-1}; 2002—2015)	n	Mean	Median
Open ocean, standard corr., white noise	10927	5.0 ± 2.0	4.9
Open ocean, standard corr., coloured noise	10927	4.9 ± 3.8	4.8
Coastal region, standard corrections	1709	4.7 ± 2.1	4.4
Coastal region, standard with FES tides	1709	4.7 ± 1.5	4.5
Coastal region, coastal corrections	1709	5.0 ± 1.5	4.9
Tide gauges with GIA VLM	63	6.5 ± 1.9	6.2
Tide gauges with SONEL VLM	23	6.2 ± 1.9	6.1

Table 2. Spatial latitude-weighted mean and median trend from the valid data set from each region and with different corrections applied. One standard error is given for the spatial mean.

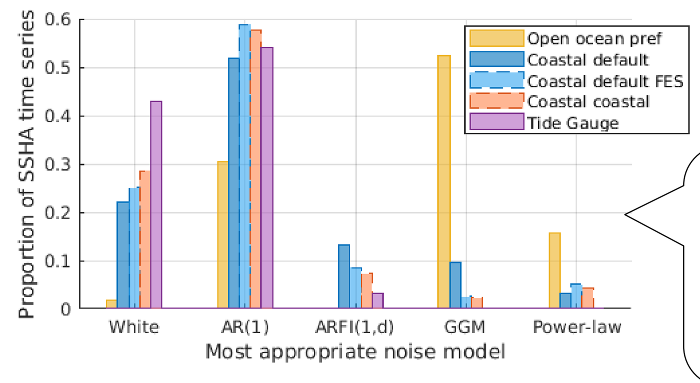

Figure 8. Most appropriate noise model from trend assessment for varying data sets.

Both the FES tidal correction and ALES range (coastal corrections) SSHA whiten or flatten the residual noise at longer periods. The trend uncertainty is reduced (c.f. standard corrections) as a result.

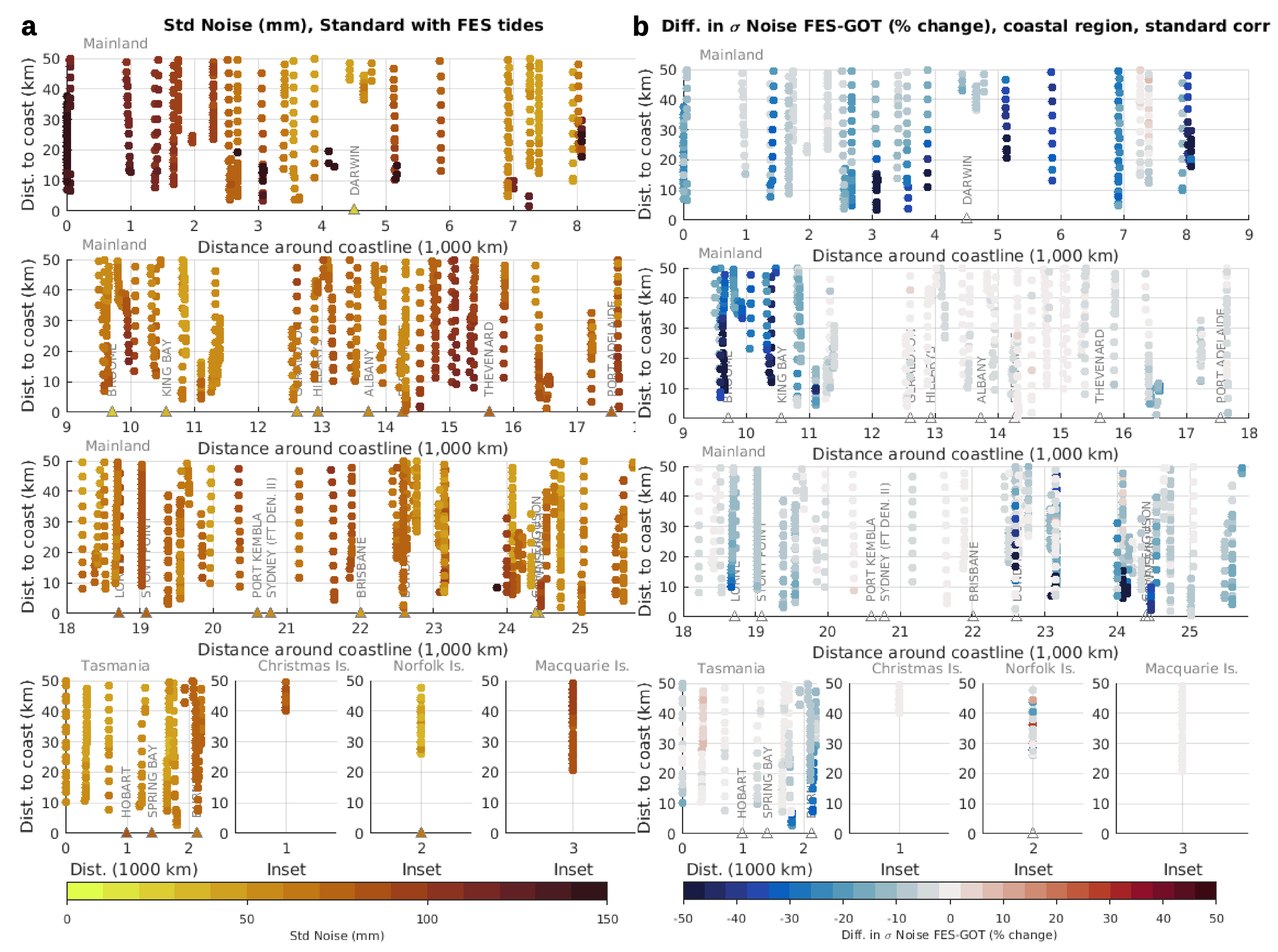

Figure 7. Standard deviation of the SSHA time series (mm): (a) standard corrections with FES tides; (b) difference (%) due to applying FES tidal correction rather than GOT

Conclusions

Linear trend and uncertainty, determined by residual noise characteristics, are investigated around the coast of Australia for new, improved coastal altimetry data sets. The data covers a very short period (2002—2015) compared with major climatic variability, so we adjust our SSHA time series by multi-variate regression with the major PDO and ENSO modes of variability.

The FES 2014b tide model gives improved variability (lower standard deviations) in the SSHA time series. SSHA calculated with the GOT tide correction exhibits greater coloured but non-AR(1) noise, which is indicative of remnant periodic power in the signal. The FES correction results in a regionally-coherent change in the trend. It is notable that the change in the trend occurs across the continental slope (>50 km from the coast).

Trends are largest in the regions of high mesoscale activity, in the East Australian and Leeuwin Currents and around Macquarie Island. The coastal altimetry corrections increase the spatial average trend in the coastal region by 0.3 mm a^{-1} (FES tides, ALES range and GPD+ wet tropospheric correction). The trend uncertainty is reduced by the coastal corrections because the variance of the SSHA time series is reduced.

In this study, trend uncertainty increases when using the most appropriate coloured noise model; the choice of noise model changes from the open ocean region (the noise is best fit by a coloured but non-AR(1) model) to the coastal region (where a white or AR(1) noise model fits best), consistent with tide gauge data. On the continental shelf, higher frequency variability can persist (due to shallow water effects and waves being supported by the coastal boundary) which lead to flatter noise profile in the power spectral density curve.